

Charge Shuttle as a Nanomechanical Rectifier

F. Pistolesi¹ and Rosario Fazio²

¹Laboratoire de Physique et Modélisation des Milieux Condensés, CNRS-UJF, BP 166, F-38042 Grenoble, France

²NEST-INFM and Scuola Normale Superiore, Piazza dei Cavalieri 7, Pisa, Italy

(Received 3 August 2004; published 27 January 2005)

We consider the charge shuttle proposed by Gorelik *et al.* driven by a time-dependent voltage bias. In the case of asymmetric setup, the system behaves as a rectifier. For pure ac drive, the rectified current shows a rather rich frequency dependent response characterized by frequency locking at fractional values of the external frequency. Because of the nonlinear dynamics of the shuttle, rectification is present also for very low frequencies. These effects could be useful to unveil the internal dynamics of nanomechanical devices.

DOI: 10.1103/PhysRevLett.94.036806

PACS numbers: 73.23.Hk, 85.35.Gv, 85.85.+j

The great burst in the study of nanoelectromechanical (NEMS) devices is unveiling several new perspectives in the realization of nanostructures where the charge transport is assisted by the mechanical degrees of freedom of the device itself. This is the case, for example, when nanomechanics [1] has been combined with single electron tunneling. Important experiments in this area are the use of a single electron transistor (SET) as a displacement sensor [2] or quantum transport through suspended nanotubes [3], oscillating molecules [4–7], and islands [8]. On the theoretical side, several works [9–20] have highlighted various aspects of the role of Coulomb blockade in NEMS.

An exciting prototype example of mechanical assisted SET device has been proposed by Gorelik *et al.* [9] and named the single electron shuttle. The authors of Ref. [9] predicted that a SET with an oscillating central island can shuttle electrons between the electrodes leading to low noise transport [10,17,18]. Although the realization of the charge shuttle is difficult experimentally, promising systems are C⁶⁰ molecules in break junctions [4,7], or silicon structures [8,21].

One of the advantage of this self-oscillating structure is the fact that one can generate very high frequency mechanical oscillation with static voltages. The fact that the system has an intrinsic and stable oscillating mode as the result of a static voltage suggests that the application of an oscillating voltage may lead to new interesting effects, related to the interplay between the external ac drive and the internal frequency of the device. Moreover, as the nonlinearities of the dynamics have an important role, this interplay should emerge in a wide interval of the ratio of the two frequencies. The aim of this Letter is to study a shuttle driven by a time-dependent applied bias. The most interesting situation is when the system is asymmetric. The structure acts as a rectifier. This behavior resembles that of ratchets [22] with a periodic forcing potential generated in a self-consistent way. We study in some details the case in which the external bias is ac and report a quite rich behavior as a function of applied frequency. We find clear indications of frequency locking. The resulting direct current may have both signs, depending on the value of the

frequency. The response to an ac field can give strong indications on the motion of the central island, even when the system is very far from the shuttling instability. A sizeable rectification is present down to frequencies much smaller than the mechanical resonating frequency. In a very recent experiment, Scheible and Blick [21] already observed similar results to those presented in our work.

The single electron shuttle, shown in Fig. 1, is a SET where the central island can oscillate between the two leads [9]. The central island is subject to an elastic recoil force, a damping force due to the dissipative medium, and an electric force due to the applied bias. The island is connected to the left and right leads through tunnel junctions with resistances $R_{L/R}(x) = R_{L/R}(0)e^{\pm x/\lambda}$ (λ is the tunneling length and x is the displacement from the equilibrium position in absence of any external drive). The capacitances C_g and C couple the island to the gate and to the two leads, respectively, and depend weakly on x in first approximation. The system is biased symmetrically at a voltage $V(t)$ ($V_R = -V_L = V/2$), the charging energy is $E_C = e^2/2C_\Sigma$, where e is the electron charge, $C_\Sigma = C_g + 2C$, and the gate charge Q_g is $C_g V_g$. For simplicity, we consider the case of low temperatures ($T \ll E_C$), charge

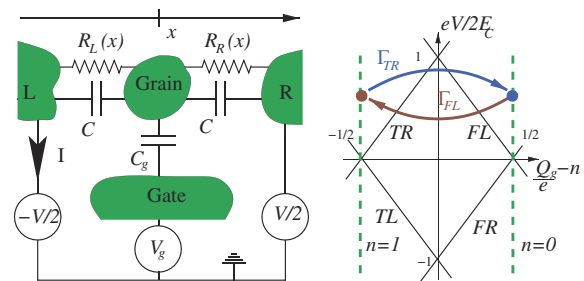


FIG. 1 (color online). Left panel: Schematic of a charge shuttle. Right panel: Energy diagram for the SET. The diagonal lines indicate the thresholds for the vanishing of the four rates Γ_{FL} , Γ_{FR} , Γ_{TL} , and Γ_{TR} . The two dots indicate the state of the system during shuttling at fixed voltage V .

degeneracy ($Q_g = e/2$), and voltages $|V| < E_C/e$. In this regime the grain can accommodate only $n = 0$ or one additional electron (see right panel of Fig. 1). We also assume that typical driving frequencies ω are small compared to $T/\hbar \ll E_C/\hbar$. This (rather weak) condition on the frequency (typically $E_C/\hbar \sim 10$ THz) allows a simple description of the tunneling in terms of time-dependent rates (see below). All the properties of the nanomechanical rectifier we want to discuss are captured already at this level. The description is quite accurate for silicon structures. The last approximation ($\hbar\omega \ll E_C$) may be rather crude to describe oscillating molecules (as in Ref. [4]), where the effects of the bias time dependence described for static SET's could become important [23,24].

In the simplest approximation the dynamics of the central island is described by Newton's law [9]:

$$\ddot{x}(t) = -\omega_o^2 x(t) - \gamma \dot{x}(t) + \frac{eV(t)}{mL} n(t). \quad (1)$$

Here m is the mass of the grain, ω_o is the oscillator eigenfrequency, γ is a damping coefficient, and L is the distance between the two leads. We refer to Ref. [9] for a detailed discussion of the validity of this phenomenological model. In the regime of incoherent transport the (stochastic) evolution of the charge $-en(t)$ is governed by the following four rates [25]: $\Gamma_{FL} = |eV(t)/4E_C| \Gamma_L(x) \Theta(V)$ and $\Gamma_{FR} = |eV(t)/4E_C| \Gamma_R(x) \Theta(-V)$ for $n = 0 \rightarrow 1$ transitions; $\Gamma_{TL} = |eV(t)/4E_C| \Gamma_L(x) \Theta(-V)$ and $\Gamma_{TR} = |eV(t)/4E_C| \Gamma_R(x) \Theta(V)$ for $n = 1 \rightarrow 0$ transitions. Here FL , FR , TL , and TR stand for from/to and left/right, indicating the direction for the electron tunneling associated to the corresponding rate, $\Gamma_{L/R}(x) = [R_{L/R}(x)C]^{-1}$, and $\Theta(t)$ is the Heaviside function. The current I is then determined by counting the net number of electrons that have passed through the shuttle in a given time t . At low temperatures the fluctuating force associated to the dissipation term $\gamma \dot{x}$ ($\int dt \langle \delta f(t) \delta f(0) \rangle \propto m\gamma k_B T$) is negligible with respect to that due to the fluctuation in the occupation number of electrons ($\int dt \langle \delta f(t) \delta f(0) \rangle \propto (eV/L)^2 \Gamma^{-1}$).

In most of the Letter, we consider the case of an oscillating voltage bias $V(t) = V_o \sin(\omega t)$, where the interplay of the two frequencies ω and ω_o is crucial. If the system is perfectly symmetric, no direct current can be generated, since this would break the left/right symmetry. We then concentrate on the asymmetric case $R_R(0)/R_L(0) \neq 1$. Charge pumping in SET devices has been already discussed in Refs. [23,24]. Note, however, all the effects discussed in this Letter are of pure electromechanical origin. None of them would exist in a SET without a moving island. Indeed we consider a symmetric bias; in this case a static SET does not lead to pumping. We performed simulation of the stochastic process governed by the four rates defined above and by Eq. (1). The results presented are obtained by simulating 10^6 events of tunneling for each plotted point. After a transient time the system reaches a stationary behavior. In Fig. 2 we

show the stationary direct current as a function of the frequency of the external bias. The rich structure shown in the figure is generic; we observed a qualitatively identical behavior in a wide range of parameters. Since our system is nonlinear, the external driving will affect the dynamics also for values of ω very different from the natural frequency ω_o . Note that in this model the nonlinearities are intrinsic to the shuttle mechanism. They are not due to a nonlinear mechanical force, but they stem from the time dependence of $n(t)$. As it is evident from Fig. 2 the rectification is present also in the adiabatic limit $\omega/\omega_o \ll 1$. In addition, we find a series of resonances due to frequency locking [26] when $\omega \approx \omega_o q/p$, with q and p integers. In this case the motion of the shuttle and the oscillating source become synchronized in such a way that every q periods of the oscillating field the shuttle performs p oscillations. In Fig. 2 we also report the low frequency current noise (lower inset). The net direct current results from large cancellations between positive and negative contributions. But the current noise is always positive, thus it does not cancel. We find that the noise remains very close to the value for a static SET (averaged over a period), $S = (2e^2/\pi) \Gamma_L \Gamma_R (\Gamma_L^2 + \Gamma_R^2) / (\Gamma_L + \Gamma_R)^3$, shown with a dashed line in the lower inset of Fig. 2. At resonance, more ordered transport is realized and current becomes less noisy [17]. In the following, we solve the problem analytically in some tractable limits, and we describe the frequency locked state.

If the electric force is much smaller than the mechanical one, $\epsilon = eV_o/(\omega_o^2 m \lambda L) \ll 1$, one can take into account the force generated by the stochastic variable $n(t)$ only on

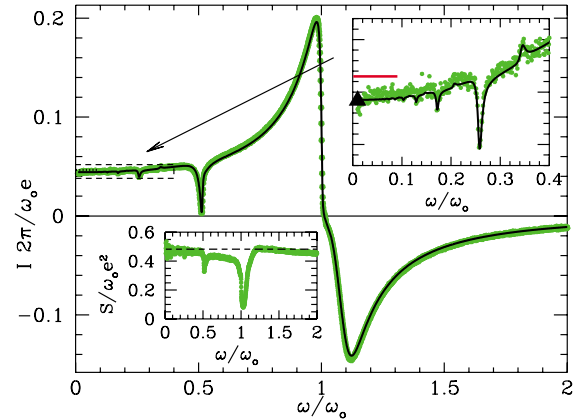


FIG. 2 (color online). Current as a function of the frequency for $\epsilon = 0.5$, $\gamma/\omega_o = 0.05$, $\Gamma/\omega_o = 1$, and $R_R/R_L = 10$. The result of the simulation of the stochastic dynamics (grey or green points) is compared with the approximate I_a (solid line). In the small frequency region, enlarged in the upper inset, several resonances at fractional values of ω_o appear. We also show (horizontal dark grey or red line) the analytical result from Eq. (4) in the adiabatic limit. The triangular dot indicates the numerical solution of the adiabatic equations. Lower inset: Current noise from the simulation (grey or green points) and analytic result (dashed line) for the static SET.

average by substituting into Eq. (1) its mean: $\langle n(t) \rangle = P(t)$, where $P(t)$ is the probability to have occupation $n = 1$ in the grain. The charge dynamics in the central island is then described by a simple master equation [25]:

$$\dot{P}(t) = -\Gamma_1(t)P(t) + \Gamma_2(t), \quad (2)$$

with $\Gamma_1(t) = |eV(t)/4E_C|(\Gamma_L[x(t)] + \Gamma_R[x(t)])$ and $\Gamma_2(t) = |eV(t)/4E_C|(\Gamma_L[x(t)]\Theta[V(t)] + \Gamma_R[x(t)]\Theta[V(t)])$. The rates depend on the time t through the voltage $V(t)$ and the position of the grain $x(t)$. The instantaneous (average) current through the structure is

$$I_a(t)/e = [1 - P(t)]\Gamma_{FL}(t) - P(t)\Gamma_{TL}(t), \quad (3)$$

where the subscript in the current indicates that the fluctuations of the force acting on the shuttle, due to the discrete nature of the charge tunneling, are neglected. As shown in Ref. [9] the shuttle instability, at constant bias, is controlled by the ratio $\epsilon/(\gamma/\omega_o)$; we can thus assume both ϵ and γ/ω_o small, but their ratio arbitrary.

In the adiabatic limit ($\omega \ll \omega_o$ and $\epsilon\omega_o/\gamma \ll 1$) it is possible to find an approximate solution of Eqs. (1) and (2). In this case the position of the grain is given by the local stationary solution of Eq. (1), $x/\lambda = \epsilon\Gamma_2(x, V)/\Gamma_1(x, V)$. Solving this equation in lowest order in ϵ , one obtains

$$I_a(\omega \ll \omega_o) = \epsilon \frac{V_o^2 e^3}{32E_C^2} \frac{\Gamma_L \Gamma_R (\Gamma_L - \Gamma_R)}{(\Gamma_R + \Gamma_L)^2}. \quad (4)$$

The corresponding value is shown in Fig. 2. The (small) difference with the full numerics is due to the additional expansion in ϵ leading to Eq. (4). By solving numerically the equation for the local equilibrium position of the grain, one obtains the result indicated by the triangular dot at $\omega = 0$ in the inset of Fig. 2 [27]. If $\epsilon\omega_o/\gamma$ is much larger than the critical value for shuttling, the behavior is completely different. The grain will oscillate at its natural frequency ω_o with the amplitude slowly modulated by $V(t)$. The modulation will be small, since for small ϵ the effect of a change in the value of V affects the mechanical motion only after several oscillations. In this case the rectified current is strongly suppressed as compared to the adiabatic limit.

We now discuss in more detail the dependence of the current on the external frequency. The most prominent structure, observed also in the experiments of Ref. [21], is present in our simulations at $\omega \approx \omega_o$, and it corresponds to the main mechanical resonance. The current changes sign across the resonance. This behavior is due to the phase relation between the driving voltage and the displacement of the grain. We verified this conjecture by solving Eq. (2) with $x(t) = A \sin(\omega t + \phi)$. By calculating the current as a function of ϕ and by means of the usual resonant dependence for $\phi(\omega) = \arctan[\omega\gamma/(\omega_o^2 - \omega^2)]$, we could reproduce qualitatively the behavior of Fig. 2.

From Fig. 2 it is clear that additional structures appear also for $\omega \approx \omega_o/q$ (magnified in the upper inset), with $q = 2, 3, \dots$ (the numerical results indicate that, except for

the fundamental frequency, even q are favorite with respect to odd ones). As we already anticipated, the motion of the shuttle and the oscillating source become synchronized at commensurate frequencies whose ratio is p/q . This ratio, known also as the winding number, can be defined more precisely as

$$w = \lim_{t \rightarrow \infty} \theta(t)/\omega t, \quad (5)$$

where $\theta(t)$ is the accumulated angle of rotation of the representative point (\dot{x}, \ddot{x}) [$\theta(t)/2\pi$ gives the number of oscillations performed by the shuttle during the time t]. When the system is frequency locked at a winding number w , it is possible to define the phase shift $\phi(t) = \theta(t) - w\omega t$. After a transient time for perfect locking, ϕ should not depend on t (apart from a small fluctuation if the motion is not perfectly harmonical). An additional important quantity to analyze is thus the phase shift variance $(\Delta\phi)^2 = \langle \phi^2 \rangle - \langle \phi \rangle^2$. This is calculated by sampling 20 points per cycle over 10^3 cycles. For a given w the smaller the value of $\Delta\phi$, the better the system locks to that external frequency. The numerical results for w and $\Delta\phi$ are shown in Fig. 3.

In Fig. 3 we show the dependence of the winding number as a function of the external frequency (top panel) together with the analysis of $\Delta\phi$ (lower panel) calculated from the stochastic simulation, line (ii), and from the average approximation, line (i). The locking at rational winding numbers is confirmed by the presence of plateaus of decreasing width. As expected the most stable plateau is at $w = 1$: the system locks very well at this frequency. We find that this holds up to very high frequency in the average approximation, where $w = 1$ seems the only possible winding number. The stochastic simulation would indicate

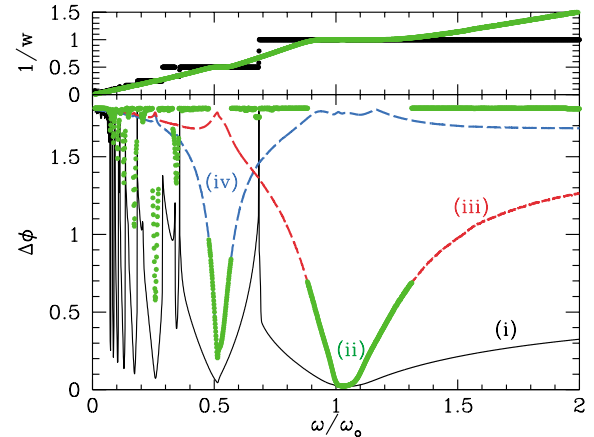


FIG. 3 (color). The top panel shows the calculated winding number obtained by the stochastic simulation (green points) and by the average approximation of Eq. (2) (black points). The bottom panel shows $\Delta\phi$ obtained with different methods: (i) average approximation (solid line), (ii) stochastic simulation with w from Eq. (5) (green points), (iii) stochastic simulation with w set equal to 1 (red dashed line), or (iv) with $w = 2$ (blue dashed line). Parameters are the same as in Fig. 2.

instead that for $\omega/\omega_o \gtrsim 1.3$ the locking with $w = 1$, as defined from Eq. (5), is no more established. We verified that this upper limit to the $w = 1$ plateaux depends essentially linearly on the asymmetry R_R/R_L . Quite generally, plateaux size increases by increasing the asymmetry. However, by studying $\Delta\phi$ for $w = 1$ in the whole frequency range, one actually obtains that a correlation is always present (i.e., $\Delta\phi < \pi/\sqrt{3} \approx 1.81$) even when Eq. (5) gives a value of w different from one. The stochastic fluctuations thus unlock the shuttle globally, but not locally. Looking at the presence of local locking at other winding numbers, we find that, for instance, $w = 2$ is clearly present for $\omega > 1$, and reversely $w = 1$ is present around $\omega = 1/2$ [see dashed lines (iii) and (iv) in lower panel of Fig. 3]. For global locking, only one phase variance is minimal. It corresponds to the “dominant” winding number. The presence of correlations of other winding numbers may indicate partial locking at these winding numbers (as in the region $0.6 \lesssim \omega \lesssim 0.9$ for $w = 1$ and 2) or the contribution of higher harmonics of $x(t)$ (as in the region $\omega > 1$).

The dependence of the phase shift around each resonance is also remarkable. It is very similar to the behavior of a forced harmonic oscillator, but instead of evolving from 0 to π it goes from ϕ_o to $\phi_o + \pi$, where ϕ_o depends on the resonance. With the aim of understanding the behavior of the current close to the resonances, we also considered the adiabatic limit and looked for harmonic oscillations superimposed to the adiabatic solution given before. This can be verified numerically by searching a periodic solution of period $2\pi/\omega$ for $P(t)$. We find that in this case the direct current is nonvanishing and that it depends strongly on ϕ . Using the phase dependence given by the full numerical calculation we could reproduce the shapes of the resonances.

All the results obtained here can be tested experimentally. Indeed a very recent paper by Scheible and Blick [21] already reports on some of the properties related to the main resonance, although no direct quantitative comparison can be made as the experiment was performed at room temperature. We discuss instead the Coulomb blockade regime which is actually a widely experimentally accessible range ($E_C \approx 80$ K in the experiment). Nevertheless, a qualitative comparison seems to indicate that the main features are present even when the Coulomb blockade is not completely established. It is worth mentioning that for the parameters of Fig. 2 the I - V characteristics presents a minimum at $\omega = \omega_o/2$ that can be made vanishing by tuning slightly the asymmetry ($R_R/R_L \approx 8$). The device could then be exploited as a sensitive frequency detector.

We thank F. Faure and A. Romito for very useful discussions. We acknowledge financial support from CNRS

through Contract No. ATIP-JC 2002 (F. P.) and EU-RTN-Nanoscale, PRIN-2002, Fibr (R. F.).

-
- [1] A.N. Cleland, *Foundation of Nanomechanics* (Springer, Heidelberg, 2002).
 - [2] R.G. Knobel and A.N. Cleland, *Nature (London)* **424**, 291 (2003).
 - [3] B.J. LeRoy *et al.*, *Appl. Phys. Lett.* **84**, 4280 (2004); P. Jarillo-Herrero *et al.*, *Nature (London)* **429**, 389 (2004).
 - [4] H. Park *et al.*, *Nature (London)* **407**, 57 (2000).
 - [5] R.H.M. Smit *et al.*, *Nature (London)* **419**, 906 (2002).
 - [6] S. Kubatkin *et al.*, *Nature (London)* **425**, 698 (2003).
 - [7] A.N. Pasupathy *et al.*, *cond-mat/0311150*.
 - [8] A. Erbe *et al.*, *Phys. Rev. Lett.* **87**, 096106 (2001).
 - [9] L.Y. Gorelik *et al.*, *Phys. Rev. Lett.* **80**, 4526 (1998); A. Isacsson *et al.*, *Physica (Amsterdam)* **255B**, 150 (1998).
 - [10] C. Weiss and W. Zwerger, *Europhys. Lett.* **47**, 97 (1999).
 - [11] D. Boese and H. Schoeller, *Europhys. Lett.* **54**, 668 (2001).
 - [12] S. Braig and K. Flensberg, *Phys. Rev. B* **68**, 205324 (2003).
 - [13] S. Sapmaz *et al.*, *Phys. Rev. B* **67**, 235414 (2003).
 - [14] T. Novotný, A. Donarini, and A.-P. Jauho, *Phys. Rev. Lett.* **90**, 256801 (2003).
 - [15] D. Fedorets *et al.*, *Phys. Rev. Lett.* **92**, 166801 (2004).
 - [16] A.D. Armour, M.P. Blencowe, and Y. Zhang, *Phys. Rev. B* **69**, 125313 (2004).
 - [17] This can be seen in the full counting statistics [F. Pistolesi, *Phys. Rev. B* **69**, 245409 (2004)].
 - [18] T. Novotný *et al.*, *Phys. Rev. Lett.* **92**, 248302 (2004).
 - [19] N.M. Chtchelkatchev, W. Belzig, and C. Bruder, *Phys. Rev. B* **70**, 193305 (2004).
 - [20] Ya. M. Blanter, O. Usmani, and Yu. V. Nazarov, *Phys. Rev. Lett.* **93**, 136802 (2004).
 - [21] D. V. Scheible and R. H. Blick, *Appl. Phys. Lett.* **84**, 4632 (2004).
 - [22] For a review, see P. Hänggi and R. Bartussek, *Nonlinear Physics of Complex Systems*, Lecture Notes in Physics Vol. 476, edited by J. Parisi, S.C. Muller, and W. Zimmermann (Springer, Berlin, 1996), p. 294; P. Reimann, *Phys. Rep.* **361**, 57 (2002).
 - [23] C. Bruder and H. Schoeller, *Phys. Rev. Lett.* **72**, 1076 (1993).
 - [24] L. P. Kouwenhoven *et al.*, *Phys. Rev. B* **50**, 2019 (1994).
 - [25] D. V. Averin and K. K. Likharev, *Mesoscopic Phenomena in Solids*, edited by B. L. Altshuler, P. A. Lee, and R. A. Webb (North-Holland, Amsterdam, 1991).
 - [26] See, for instance, R. C. Hilborn, *Chaos and Nonlinear Dynamics* (Oxford University Press, New York, 2000).
 - [27] Rectification can also be detected by injecting low frequency noise in the system. The resulting current, in the low frequency regime, $I_a = \epsilon(e^3 P_V / 4E_C^2) \Gamma_L \Gamma_R (\Gamma_L - \Gamma_R) / (\Gamma_R + \Gamma_L)^2$ is proportional to the integrated power spectrum of the noise $P_V = \langle V^2 \rangle$.